

A STUDY OF RADIANT ENERGY AND GASEOUS EMISSION OF INFRARED BURNERS

T. Bai, Y. D. Yeboah, J. X. Nie, Z. Wang, J. Shang
Combustion and Emission Control Laboratory
Clark Atlanta University
Atlanta, Georgia 30314

ABSTRACT

An infrared (IR) burner is one of the fully primary aerated burners and a surface combustor that elevates the temperature of the burner head to a radiant condition. Because of their energy-efficiency and environmental characteristics, infrared burners are receiving more and more interest. However, infrared burners are not yet as well characterized as the partially aerated blue flame burners.

Using an innovative measurement setup, infrared radiation from an infrared burner was measured along with its emissions. The infrared spectrum from the burner was found to cover the IR range from 6500 to 450 cm^{-1} and concentrates its spectral intensity in the 4000 to 500 cm^{-1} wavenumber range with strong H_2O absorbances at 2000 - 1400 and 3700 - 3650 cm^{-1} , and CO_2 absorbances at about 2350, 2330 and 667 cm^{-1} . The radiant energy was proportional to the integration of the measured spectrum within the wavenumber range. To quantify the total infrared energy from the burner a blackbody was used to calibrate the FTIR. The infrared spectrum from an infrared blackbody covers the range of 6500 - 450 cm^{-1} . The radiant energy from a blackbody depended on its temperature alone. Further more, with certain corrections, the radiant energies of an infrared burner was calculated from the measured infrared data by using the blackbody as a standard.

At the equivalence ratio $\Phi = 1$, the radiant efficiency of the infrared burner reached its maximum, ~31.4%. As the equivalence ratio shifted away toward either fuel-lean or fuel-rich side, the radiant efficiency was quickly decreased. The addition of nitrogen to the premixed methane-air combustion caused the gas dilution so that it decreased the radiant efficiency. The addition of the propane to the premixed methane-air combustion did not affect the radiant efficiency. The hydrogen addition increased the radiant efficiency. Emission studies indicated that the emission gases CO_2 and NO_x also reached its maximum value of 10.7% and 8 ppm at $\Phi = 1$, respectively. The concentration of NO_x produced from an infrared burner was significantly lower than that produced from a conversational burner.

INTRODUCTION

An infrared (IR) burner is one of the fully primary aerated burners which have been introduced more recently. The infrared burner is a surface combustor that elevates the temperature of the burner head to a radiant condition. A variety of metallic and ceramic materials are used for the burner heads. The ceramics offers an attractive choice for these burners because of their high temperature resistance capabilities. These burners have a submerged flame allowing better convective heat transfer between the solid phase and the gas phase [1]. A large porous surface area to volume ratio of the solid matrix results in an enhanced heat transfer between the gaseous and

the solid phase. The matrix is at a high temperature in the preheat region due to radiation and conduction transfer upstream from the reaction zone. The incoming fuel air mixture is preheated and the ranges of flammability and flame stability may be substantially extended to the equivalence ratios of 0.6 - 0.7 [1].

The principle of recirculating heat from hot products to cold reactants by heat exchange without intermixing the gases was first introduced by Weinberg [2]. These burners have an increased combustion rate and thermodynamic efficiency for energy conversion and heat transfer. Theoretical and experimental studies were performed by Takeno and his co-workers [3, 4]. A wide range of radiation efficiencies (varying from 15% to 50%) have been reported in the literature for similar operating conditions for the radiant burners [1, 5-7]. A number of researches have experimentally investigated the pollutant emission from radiant burners [7-9]. A comprehensive review of combustion within porous inert media is available in the literature [10, 11]. However, infrared burners are still not yet as well characterized as the partially aerated blue flame burners. They have been developed along an empirical path by individual manufacturers to use minimum air to achieve the maximum flame temperature and at the same time maintain stable combustion. Although this design can achieve high intensity radiation, it sacrifices the flexibility of a burner with high aeration. In service, they have had reliability and performance problems, especially when exposed to various gas compositions, operating altitudes and other ambient conditions. This results in sensitivity of its performance to fuel composition changes and other factors.

The burner used in this study is installed in a commercial McDonald's deep fat fryer. It consists of a fan powered air supply, an air/fuel mixing chamber, and a porous ceramic radiant tile, see Fig. 1. Combustion takes place on the surface of the perforated ceramic tile creating a radiant heat source. This is attributed to the fact that a large proportion of the heat of combustion is given out as radiation from the burner surface, and results in relatively low gas temperature in the combustion zone compared to that of a conventional free-flame burner, so that infrared burners produce low CO and NO_x emissions in a controlled geometric space [3, 8, 12].

Pollutant emissions have been one of the most important issues in combustion research in the last few decades [13]. NO_x, NO + NO₂, is harmful to human health when inhaled, damages vegetation, and degrades materials through acid deposition [13-16]. When illuminated by sunlight, atmospheric NO reacts with gaseous hydrocarbons and O₂ to form photochemical oxidants, such as peroxyacetal nitrate (PAN) and ozone [17]. Emission of NO_x into the atmosphere may be responsible for the inability of large metropolitan areas to meet the National Ambient Air Quality Standards for O₃ [18]. Exhaust gases from the combustion of fossil fuels are one of the major sources of anthropogenic NO_x. In 1985, 18.6 × 10⁶ metric tons of NO_x was released into the atmosphere by human activities in the United States [19]. Combustion processes contribute ≈ 10.6 × 10⁶ metric tons of NO_x annually, which accounts for 57% of the total anthropogenic emission from the US for 1985 [19]. Infrared burners produce low NO_x and CO emissions in a controlled geometric space. As the environmental regulations become more stringent [20], infrared burners are receiving more and more interest [1, 21, 22].

The performance of natural gas-fired radiant burners is strongly dependent on ambient conditions and natural gas composition. In the United States, ambient temperature, pressure, and relative humidity vary significantly by location and season. Also, natural gas compositions supplied by local gas distribution companies exhibit seasonal and regional variations. These variations can cause reliability and performance problems in gas-fired equipment. In service, IR burners have had reliability and performance problems, especially when exposed to various gas compositions, operating altitudes, and other ambient conditions like temperature and humidity. These parameters also affect the composition of the gaseous emissions from these burners. Burning characteristics will differ in important respects, one of the most being speed of flame propagation. It is the responsibility of the manufacturers to design appliances capable of performing more satisfactorily under reasonably wide variations in gas composition while retaining desirable efficiencies and operation.

There have been very limited studies to investigate the effects of gas composition upon the performance of radiant burner. Due to the lack of data and fundamental understandings, the IR burner product development in the industry is empirical in nature, and is conducted with one gas composition. This study characterizes the operation of IR burner at various gas compositions and ambient conditions and develops a baseline theoretical analysis to predict the behavior of these burners to the change in fuel compositions.

EXPERIMENTAL

Experimental Setup

An experimental setup consisted of a gas feed system, a commercial deep fat fryer (combustor), a radiation measurement system, and an exhaust gas sampling and measurement system, see Fig. 1.

Commercial-grade cylinder methane (>93.0% CH₄) produced by C&C Oxygen Co. (Chattanooga, TN), and zero-grade nitrogen (>99.999% N₂), high-grade propane (>99.9% C₃H₈) and ultra-high grade hydrogen (>99.99% H₂) produced by Fil Holox Inc. (Atlanta, GA) were used. The gaseous flow rates and the fuel/air ratios were

precisely controlled by an MKS gas mass-flow control system (1179 A Mass-Flo Control, MKS Instruments Inc.), which consisted of a 50-slm (methane), a 200-slm (air), and a 5-slm (nitrogen/propane/ hydrogen) mass flow controller, and a 647B multi gas controller.

The burner used for this study was a commercial deep fat fryer. The hearth of the burner was made by two parallel and vertical-mounted porous ceramic tiles. Each ceramic tile has a dimension of 35 × 18.5 cm (length × width), and ~19,500 small even-distributed holes. The hole had an 1-mm inner diameter and a 14-mm depth. At the typical gas flow of this study, 100 slm, the Reynolds number for the combustion (through the hole) is calculated as 7.5, which is in a laminar flow region. The burner was modified to allow in-situ radiation measurements on the surface of the infrared burner via a view port installed on the side wall of the oil vat. Experiments were conducted for an extensive test matrix of fuel-air mixtures. The total gas flows used were varied from 70 to 200 dm³/min. The typical fuel flow used was 8 dm³/min. The equivalence ratio Φ was changed by changing the air flow rate.

Radiant Energy Measurements

A Perkin-Elmer Spectrum 2000 FTIR spectroscopy system (Perkin-Elmer Co., Norwalk, CT), consisting of a 15798.01 cm⁻¹ reference laser, an external source and an internal (temperature stabilized wire coil) source options, a 12.50 mm Jacquinot-stop aperture with the resolution of 6.48 cm⁻¹, an interferometer with a beamsplitter of 6500 - 450 cm⁻¹, and an air-cooled triglycine sulfate detector (TGS, 15600 - 200 cm⁻¹), was used for the radiation measurement. The TGS detector has a better background contribution compared to other kinds of detectors, which is important for the wide-band radiation measurement. Perkin-Elmer Spectrum for Window version 1.0 software was used for spectral manipulation. All radiation measurements were conducted by using the measured body (gas burner) as the external source. The effective aperture window size for the external source and the distance between the external source and instrumental interferometer were precisely controlled. For reducing the fluctuation of test conditions, 4 scans were co-added for each spectra with a nominal resolution of 8 cm⁻¹ in the range of 6500 - 450 cm⁻¹. Before the radiation measurements, the instrument was warmed for more than two hours and automatically tuned up for the maximum sensitivity, then a background spectrum was taken. The radiation-measurement spectral manipulation such as baseline correction and subtraction were made from the background measurement. Since the radiant signals were very strong, (the measurement noises were relatively small), the spectra were presented and used for the radiant calculation without further noise reduction and smoothing. The FTIR spectroscopy was calibrated for the radiant energy calculation by using a Graseby Infrared 564 blackbody (Graseby Co. Orlando, Florida).

By using the CO₂ infrared peaks as an internal standard, the measured infrared spectra of the IR burner were averaged and corrected to reduce the errors. The corrected infrared spectra of the IR burner were integrated and converted to the radiant energy according to the blackbody's infrared spectra. The detail procedures were reported in references 23 and 24.

Emission Measurements

An exhaust analysis system, consisting of six commercial Horiba gas analyzers (Horiba Instruments Inc., Irvine, CA) and a lab-made sampling manifold, was used to collect exhaust gases for CO, CO₂, O₂, NO_x and total unburned hydrocarbon (UHC) analyses. The gas analyzer was calibrated with gases of known composition. The exhaust gas sample was continuously taken through a ¼ -inch stainless steel tube from the chimney of the burner. The tip of the sampling tube was placed in the middle of the burner chimney (about 5 inch deep from the opening of the chimney). A chillier-trap was used to condense the water out before the sample entered the species analyzer. Traditionally, a sample gas was taken by a vacuum sampling pump of an analyzer. The whole sampling system was running in the vacuum condition, which made it easy for air to leak into the sample gas. Therefore, a gas pump was connected to the very beginning of the sampling tube to convert the sample gas in the sampling system from a negative pressure (vacuum) to a positive pressure, which significantly reduced the air leaking into the sample gas and increased the measurement reliability. CO and CO₂ were analyzed by the Horiba VIA510 gas analysis units, based on non-dispersive infrared methods with the measuring ranges of 0 - 5,000 ppm and 0 - 20 vol% for CO and CO₂, respectively. O₂ was measured by a Horiba MPA-510 magnetic-pressure-type-oxygen analyzer with the measuring range of 0 - 50 vol%. NO_x was analyzed by a Horiba CLA-510SS chemiluminescence analyzer with the measuring range of 0 - 2,500 ppm. The total unburned hydrocarbon (UHC) was analyzed by a Horiba FIA-510 analyzer based on the hydrogen flame ionizing method and with the measuring range of 0 - 10,000 ppm. All of the Horiba analyzers had reproducibilities of less than 0.5% of the full scales. During the emission measurements, the view port for the IR measurement were completely sealed to avoid air leakage into the combustion zone. Three measurements were made for each test condition and the average of the results from the three measurements was used for the final calculation and discussion. The relative standard deviations of three measurements for all the experiments were less than 1%.

Temperature Measurements

A 0.8-mm Ni-Cr/Ni-Al (K type) thermocouple and a model HH23 microprocessor thermometer (Omega Engineering Inc., Stamford, CT) were used for the temperatures of the flame and ceramic tile surface at the various gas flows, fuel/air ratios. Since the ceramic tile was vertically mounted, an unevenly vertical temperature distribution at the burner surface was found. Therefore, the temperatures were measured at the location of 0.5 cm above the center line of the ceramic tile and from a different distance to the tile's surface. Errors in intrusive probe and thermocouple measurements were of concern.

Experimental Methods

Experiments were conducted for an extensive test matrix of fuel gas mixtures that represented the complete range of gas compositions usually encountered in the United States. Methane was used as the baseline fuel. Mixtures of methane/propane, methane/hydrogen, and methane/nitrogen were tested to study the effect of fuel mixtures on the performance of the radiant burners. The performance of the burner is investigated in terms of radiant efficiency and gaseous emissions at various gas compositions and air/fuel ratios. The total gas flows used were varied from 70 to 200 slm. The typical fuel flow used was 8 slm. The equivalence ratio Φ was changed by changing the air flow rate.

RESULTS AND DISCUSSION

Radiant Measurements

Spectrum of Infrared Burner

The infrared spectrum from a commercial deep fat fryer, shown in Fig. 2, covers the IR range from 6500 to 450 cm^{-1} and concentrates its spectral intensity in the 4000 to 500 cm^{-1} wavenumber range with strong H_2O absorbances at 2000 - 1400 and 3700 - 3650 cm^{-1} , and CO_2 absorbances at about 2350, 2330 and 667 cm^{-1} [25-27], respectively. The magnitudes of the measured spectra within the wavenumber range were proportional to the energy which was put into the combustion, see Fig. 3, so the spectra can be used for the calculation of the radiant energy from the burner.

Figure 4 shows that an infrared spectrum of a blackbody was similar to that of the infrared burner. The two spectra well overlapped with each other almost in whole mid infrared band, except for the CO_2 absorbance peaks at 2350 and 2330 cm^{-1} , as shown in Fig. 4. This is because the blackbody was heated by electricity. The CO_2 absorbance was from the atmospheric CO_2 , which was measured to be only about 0.04% by volume [23, 24]. On the other hand, the infrared gas burner was burned by methane in air, where up to 12% of CO_2 was presented [12].

Radiant Energy Measurements

Figure 5 shows the IR radiant energies measured at different equivalence ratio Φ , which is defined as the ratio of the actual fuel-air ratio to the theoretical fuel-air ratio. It can be seen that in the fuel-lean combustion region as the equivalence ratio increased from 0.55 to 0.95, the radiant efficiency increased from 0.14 to 0.3. At $\Phi \approx 1$, where the stoichiometric fuel-air ratio for combustion was closed, the radiant efficiency reached its maximum, ~31.4%. This value is close to the radiant efficiency obtained by Mital and Gore from a much smaller (45 cm^2) laboratory radiant burner [1]. After passing $\Phi = 1$, the combustion took place in the fuel-rich combustion region. As Φ was further increased from 1.1 to 1.3, the radiant efficiency decreased from 0.3 to 0.27 due to the excess air. Figure 5 shows that in an equivalence ratio range from 0.95 to 1.1 the radiant efficiency of the combustion did not change much. This is believed to be caused by air leaking from opened-to-the-atmosphere view port for the radiation measurement. In order to confirm this air leakage effect, a glass window was used to seal the open view port so that the measurement was made by passing the infrared radiation through the glass window. Although because of glass's strong absorbance in some IR bands, the measured absolute spectral magnitudes were distorted and much lower than those without the glass window, the results in Fig. 8 does show that radiant efficiency was much more sensitive to the equivalence ratio and reached its maximum value at $\Phi = 0.98$.

Temperature Measurements

The temperatures of the combustion were measured from different locations inside/outside ceramic tile. Under the typical experimental conditions of this study (i.e. 8.0/76 slm of methane/air, $\Phi = 1$), the highest temperature of the flame was found to be about 900 °C and located at the place of about 2 mm from the ceramic tile surface, as shown in Fig. 6, which was similar to the reports from the literature [1, 8]. This temperature is about 100 °C higher than the temperature on the tile surface (Fig. 6). It should be noticed that the temperature for the methane-air combustion shown in Fig. 6 did not change much with the equivalence ratio and the maximum

temperature did not locate at $\Phi = 1$, which was probably due to the effect of the total flow change. The changes of the total flows changed the gas velocity from the small holes of the ceramic tile and the air entrainment in the burner, which resulted in the changes of the maximum temperature locations.

Effect of Nitrogen on Radiant Efficiency

Figure 7 shows that as 2.4% and 7% of nitrogen (based on the amount of methane) were added to the methane-air mixture, in the fuel-lean region, the radiant efficiency of combustion decreased by about 2% and 6%; in the fuel-rich region, the radiant efficiency decreased by about <0.5% and 2%, respectively. As a result, the maximum efficiency region shifted to the fuel-rich region. This phenomenon may be caused by the gas dilution and heat absorption. Since nitrogen is a non-combustible gas, it absorbs the energy when it is added to the combustion. In the fuel-lean region, the amount of fuel was already insufficient. The nitrogen addition further diluted the fuel so as to make the insufficiency worse. This dilution plus the heat absorption by the added nitrogen resulted in a greater nitrogen-addition effect. In the fuel-rich region, the fuel was excess, so the effect of nitrogen addition was mainly from the combustion-energy absorption. Therefore, its effect on the combustion became smaller.

Effect of Propane on Radiant Efficiency

The results in Fig. 8 indicate that the addition of propane to the methane did not affect much on the radiant efficiency of the combustion, at least in the fuel-lean combustion region. This is because propane and methane have quite similar physical and chemical property. Both propane and methane are straight chain saturated hydrocarbons at the gaseous state in the ambient temperature and pressure. They also produce the same combustion products, CO_2 and water, as shown in Eqs. 1 and 2.



When completely combusted in the air, the exhaust produced from one mole methane consists of $\text{N}_2 = 2 \times 79/21 = 7.52$ moles, $\text{CO}_2 = 1$ mole, and $\text{H}_2\text{O} = 2$ moles. The heat capacities of N_2 , CO_2 and H_2O are 29.1, 37.1, and 33.6 J/mole•K, respectively [28]. So the total exhaust gas heat capacity from one mole methane combustion is $7.52 \times 29.1 + 1 \times 37.1 + 2 \times 33.6 = 323.2$ J/K, (mole \times J/mole•K = J/K). The total exhaust gas heat capacity from one mole propane combustion is $(5 \times 79/21) \times 29.1 + 3 \times 37.1 + 4 \times 33.6 = 793.1$ J/K. The combustion enthalpies for Eqs. 7 and 8 are 890.8 and 2219 kJ/mole, respectively [28]. If the combusted heat was totally consumed by the exhaust gases and the changes of the gaseous heat capacities with temperature are omitted, the maximum exhaust gas temperature increases by combusting one mole methane and propane are $890.8 \times 1000 / 323.2 = 2756$ and $2219 \times 1000 / 793.1 = 2798$ K/mole, respectively. This means, thermodynamically, the substitution of methane with propane will not noticeably affect the molar combustion heat. (It should be mentioned that if burned with pure oxygen, propane will produce a higher molar combustion heat because its exhaust gas is reduced by $5 \times 79/21 = 18.8$ moles of nitrogen, compared to the methane's $2 \times 79/21 = 7.5$ moles of exhaust gas reduction.) Actually, however, a large amount of the combusting heat was transferred to the combustor's wall. The exhaust gases can not reach the maximum temperature. Therefore, the combustion of the propane-air produced higher temperature due to its higher molar combustion enthalpy [12].

On the other hand, for the saturated straight-chain hydrocarbons as the number of carbon increases, its stability increases, and its mass transfer rate decreases. Therefore, kinetically its ignition (combustion) becomes more difficult. Especially in the situation where the oxygen (air) insufficiency, this kinetic effect becomes stronger so that some of propane molecules could not be ignited and combusted fast enough in the combustion chamber near the surface of the ceramic tile of the burner. These unburned hydrocarbons flowed to the chimney with the emission gases and continuously combusted there. This phenomenon has been observed in the study. We believed that it is this unburned propane which resulted in the decreased radiant efficiency in the fuel-rich region.

Effect of Hydrogen on Radiant Efficiency

Fig. 9 illustrates that as 5% and 12% by volume of hydrogen (based on the amount of methane) was added to the methane-air premixed gas, the radiant efficiency of the combustion increased by about 2% and 4%. (The 2.5% of hydrogen addition was too small to see its effect.) Hydrogen was combusted as follow,



The combustion enthalpy for Eq. 3 is 241.8 kJ/mole [28]. Without heat loss to the combustor, burning one mole of hydrogen in air leads to the maximum exhaust-gas temperature increase by $241.8 \times 1000 / (0.5 \times 79/21 \times 29.1 + 1 \times 33.6) = 2737$ K. This is quite close to that from the combustion of methane. However, at first, unlike the

combustion of methane or other hydrocarbons, the hydrogen combustion does not produce an incomplete combustion product (CO), but directly combusted into its final product (H₂O), which leads to an actual higher combustion efficiency. Secondly, hydrogen molecules have lower ignition activation energy and faster mass transfer rate than methane. They can be more quickly ignited and more thoroughly combusted in the combustion chamber near the ceramic-tile surface of the burner, which leads to that the more combusted heat is absorbed by the ceramic tile and is converted to the radiant energy. These two factors result in a higher radiant efficiency for the hydrogen-air combustion.

Emission Measurements

CO₂ and O₂ Measurements

CO₂ is one of the main product of the methane-air combustion. The concentration of CO₂ in the combustion exhaust can be used to evaluate the completeness of the combustion process. In a given condition, the CO₂ concentration was found to be proportional to the combustion efficiency, see Fig. 10. Figure 10 shows that in the fuel-lean combustion region, as the equivalence ratio Φ increases from 0.5 to 1, the concentration of CO₂ in the exhaust increased from 7.5% to 10%. At $\Phi \approx 1$, where the stoichiometric fuel-air ratio for combustion was reached, the concentration of CO₂ arrived at its maximum, 10.7%. Theoretically, when a mole of CH₄ is completely combusted in air it will consume 2 moles of oxygen and produce one mole of CO₂ and 2 moles of water plus $2 \times 79/21$ moles of nitrogen. If the produced water vapor is not condensed, at the stoichiometric fuel-air ratio ($\Phi = 1$), the CO₂ concentration in the combustion exhaust should be $1/(1+2+2 \times 79/21) = 9.5\%$. On the other hand, if the water vapor is completely condensed, the CO₂ concentration should be $1/(1+2 \times 79/21) = 11.7\%$. It is believed that some of the water vapor still existed in the sampling system. Therefore, the 10.7% of the CO₂ concentration at the stoichiometric combustion may indicate complete combustion of methane in the air. This was confirmed by the analysis of the unburned hydrocarbons in the exhaust gases, see later.

CO and UHC Measurements

In the fuel-lean combustion region, where the air was in excess, the concentration of O₂ was shown to proportionally decrease as the equivalence ratio increased until to about $\Phi = 1$, where the O₂ concentration reached its lowest point, $\sim 0.2\%$ (see Fig. 5). After that, as the equivalence ratio further increased, the O₂ concentration did not effectively change but kept at about 0.2%.

In the case of the oxygen deficiency, as in the fuel-rich combustion, the CO concentration becomes significant. The experimental results in Fig. 6 indicate that in the fuel-lean combustion region, where the air in the premixed gas was excess, the CO concentration slowly increased from 240 to 320 ppm as Φ was increased from 0.75 to 1 due to the increase of the combustion temperature according to the Boudouard reaction [29],



As the temperature increases (over 700 °C), the equilibrium of Eq. 4 shifts to left side. When the combustion was moved into the fuel-rich region, the CO concentration immediately jumped to 4300 ppm at $\Phi = 1.02$. This is because in the fuel-rich region the fuel (methane) is excess, which led to the incomplete combustion. Since the instrumental measurement limitation for CO is 5000 ppm, the higher CO concentration could not be determined.

The unburned hydrocarbon (UHC) is a function of the O₂ concentration. As mentioned previously, the hydrocarbons that were not burned near the surface of the burner would be consumed further downstream. As a result, the measured unburned hydrocarbon concentration near the exit of the burner was quite close to equilibrium state. In the fuel-lean combustion region, the concentrations of the total unburned hydrocarbons increased slowly from 100 to 300 ppm as Φ increased from 0.6 to 1, as shown in Fig. 7.

NOx Measurements

NOx is mainly the mixture of NO and NO₂ [1]. Figure 12 shows that the NOx concentration was heavily dependent on the equivalence ratio, and had a maximum value of 7.5 ppm at $\Phi \approx 1$. This phenomenon may be caused by the kinetic factors, i.e., the rate of NOx formation. Since the formation rate of NOx is controlled by the kinetic factors [12], the concentrations of NOx in the exhaust gases are mainly the function of combustion temperature since the kinetic reaction rate is proportional to temperature [13]. In the region of $\Phi \approx 1$, the burner reached its highest temperature, and the burner's temperature decreased as Φ deviated from stoichiometric conditions. The shift of the NOx curves to fuel-rich region further confirmed that some of the hydrocarbons may not be burned near the tile surface of the radiant burner. This fuel-rich shift for the NOx curve was also reported from the combustion of an auto engine [30] and other liquid-fueled premixed combustion [13]. As discussed before, the maximum temperature for the combustion of this infrared radiant burner is only about 900 °C, Therefore, there are

much less NO_x formation. On the other hand, in the similar total fuel-air flow and equivalence ratio, the temperature at the hottest spots of a traditional burner were measured as ~1700 °C in our lab and ~ 1600 °C in the literature [1]. And the NO_x concentrations of the combustion exhaust from a traditional premixed methane/air burner were measured as ~60 ppm in our lab [31] and as 100 - 350 ppm from literature [1]. The NO_x produced from the infrared radiant burner was < 12% of that from a traditional gas burner. This demonstrates one of the advantages of IR radiant burners.

The effects of nitrogen, propane and hydrogen on the exhaust of the methane-air combustion are relatively small [12], except for the effect of propane addition on the NO_x formation. With 18% by volume of propane addition (based on the amount of methane), the NO_x concentration in the exhaust increased from ~8 ppm to 18 ppm, more than doubled. It is believed this is caused by the temperature increase, because it was found as 18% of propane addition, the combustion temperature increased about 100 °C, from 900 to 1000 °C [12].

CONCLUSIONS

- The commercial natural gas IR burner performed differently in the different conditions. For the methane-air combustion, at the equivalence ratio $\Phi \approx 1$, the infrared burner produced its maximum radiation efficiency, ~31.4%. This radiant efficiency was a sensitive function of the equivalence ratio of the combustion gas. As the equivalence ratio increased from 0.55 to 0.95, the radiant efficiency quickly increased from 14% to 31%. In the fuel rich region, as the equivalence ratio increased, the radiant efficiency gradually decreased. The combustion temperature of an infrared burner was much less sensitive than the radiant efficiency. In the equivalence ratio range of 0.6 to 1.3, the combustion temperature of an infrared burner varied only about 50 °C. Nitrogen addition caused the decrease of radiant efficiency mainly due to the dilution and heat consumption. The addition of propane did not affect much on the radiant efficiency of the combustion, except for the fuel rich region, where the increase of the unburned propane resulted in the decrease of the radiant efficiency. The hydrogen addition to the methane-air combustion increased radiant efficiency because of its quicker and complete combustion.
- Similar to a traditional methane-air gas burner, at the equivalence ratio $\Phi = 1$, the IR burner produced its maximum CO₂, ~ 10.7%. In the fuel-lean region, the O₂ concentration in the emission gas decreased proportionally as Φ increased, but the concentrations of CO and UHC were kept in a couple of hundred ppm ranges. In the fuel-rich region, the O₂ concentration was kept as a constant, ~ 0.2%, but the CO and UHC concentrations quickly jumped to thousands ppm or more as Φ increased. Because of the uniform temperature distribution, the IR burner produced lower combustion temperature (900 °C) and NO_x (~8 ppm) than traditional gas burners, where the combustion temperature and NO_x are generally 1700 °C and >60 ppm. Propane addition to the methane-air mixture increased the NO_x concentration in the exhaust due to the increase of the combustion temperature.

ACKNOWLEDGMENTS

This work was supported by US Department of Energy, through Contract No. DE-FG22-94MT94011 and the natural gas industry. AGA Research is our industrial partner.

REFERENCE

1. Mital, R., Gore, J. P.; Viskanta, R., and Singh, S.; "Structure of Submerged Flames in Reticulated Ceramic Radiant Burners," *the Proceedings of 30th Section Anniversary Technical Meeting, Central States Section, the Combustion Institute*, St. Louis, MR, 1996, p.310-315.
2. Weinberg, F.J.; *Nature*, 1971, 233, p.239-241.
3. Takeno, T.; Sato, K. and Hase, K.; *18th Symposium (International) on Combustion*, The Combustion Institute, Pittsburgh, PA, 1981, p.465-472.
4. Kotani, Y. and Takeno, T.; *19th Symposium (International) on Combustion*, The Combustion Institute, Pittsburgh, PA, 1982, p.1503-1509.
5. Tidball, R. K.; Donaldson, R. J. and Gotterba, J. A.; *Radiant Burner Technology Base - Burner Research and Development*, GRI Final Report No. GRI 89/0253, 1989.
6. Ruiz, R. and Singh, S. N., *Presented at the International Gas Research Conference*, Orlando, FL, 199, 2, p.2410-2419.
7. Khanna, V.; Goel, L. and Ellzey, J.L.; *Combust. Sci. and Tech.*, 1994, 99, p.133.

8. Williams, A.; Woolley, R. and Lawes, M.; "The Formations of NO_x in Surface Burners," *Combustion and Flame*, 89 (1992), p. 157-166.
9. Kulkarni, M. R.; Chavali, K. P. and Peck, R. E.; *Proceedings of the Western States Section of the Combustion Institute*, Berkeley, CA, 1992.
10. Hall, M.J. and Hiatt, J. P.; *Physics of Fluids*, 1994, 6(2), p.469-470.
11. Howell, J. R.; Hall, M. J. and Ellzey, J. L.; *Presented at the ASME Energy Sources and Technology Conference and Exhibition*, Houston, TX, 1995.
12. Bai, T.; Yeboah, Y.D.; Nie, J.X.; Wang, Z. and Shang, J.; "Low Emission Characteristics Of Radiant Burner," the proceedings of *1998 Energy Sources Technology Conference*, Houston, TX, Feb. 2-4, 1998, ETCE98-4770.
13. Tseng, L. K. and Gore, J. P.; "NO_x Emission of Confined Liquid Fueled Partially Premixed Turbulent Jet Flame," *the Proceedings of 30th Section Anniversary Technical Meeting, Central States Section, the Combustion Institute*, St. Louis, MO, 1996, p.86-90.
14. Spengler, J. D.; Brauer, M.; Koutrakis, P.; *Environ. Sci. Technol.*, 1990, 24, p. 946.
15. Gauri, K. L. ; Holdren, G. C., Jr.; *Environ. Sci. Technol.*, 1981, 15, p. 386.
16. Air Quality Criteria for Nitrogen Oxides; U.S. Department of Health, Education, and Welfare, U.S. Government Printing Office, Washington, DC, 1971.
17. Singh, H. B.; *Environ. Sci. Technol.*, 1987, 21, p.320.
18. Thomas, L. M.; EPA J., 1987, 13, (OCT), p.2.
19. The National Acid Precipitation Assessment Program, 1989, Annual Report to the President and Congress, 1989, p f-43.
20. Hanson, D. J.; "EPA Releases Toxics Inventory," *Chemical & Engineering News*, June 9, 1997, p.22-23.
21. Sathe, S. B.; Kulkarni, M.R., Peck, R.E. and Tong, T.W.; "An Experimental and Theoretical Study of Porous Radiant Burner Performance," *23rd Symposium (International) on Combustion/The Combustion Institute*, 1990, p.1011-1018.
22. Sheridan, R.; "Determination of Radiant Output from Infrared Tube Heaters," *GRI Topical Report*, May 1994.
23. Clark Atlanta University, "A Method for Measuring the Radiant Energy by an Internal-Standardized Fourier Transform Infrared Spectroscopy," US Patent applied.
24. Bai, T.; Yeboah, Y.D.; Nie, J.X.; Wang, Z. and Shang, J.; "Measurements of Radiant Efficiency of Gaseous Infrared Burners by Fourier Transform Infrared Spectroscopy," *27th International Symposium on Combustion*, Boulder, CO, Aug. 2-7, 1998.
25. Taylor, J.H.; Benedict, W.S. and Strong, J.; *J Chem. Phys.*, 20, 1952, p. 1884.
26. Nakamoto, K.; *Infrared Spectra of Inorganic and Coordination Compounds*, 2ed ed., John Wiley & Sons Inc., New York, 1970, p. 17-18, 83.
27. Plank, M.; *Vorlesungen uber die Theorie der Warmestrahlung*, 5th ed., Barth Leipzig, 1923.
28. Lide, D.R., ed.; *CRC Handbook of Chemistry and Physics*, 73rd ed., CRC Press Inc., Boca Raton, 1992, p. 10-300 - 10-301.
29. Glassman, I.; *Combustion*, 1977, Academic Press Inc., New York, p.245.
30. Nevers, N. de; *AIR POLLUTION CONTROL ENGINEERING*, McGraw-Hill Inc., New York, 1995, p.378-393, 416.
31. Yeboah, Y.D.; Bai, T.; Nie, J.X. and Shang, J.; "Effect Of Equivalence Ratio, Flow Rate And Nozzle Material On The Emission Gases Of Premixed Methane-Air Combustion," *1998 AIChE Spring National Meeting*, New Orleans, LA, March 8-12, 1998, paper 87d.

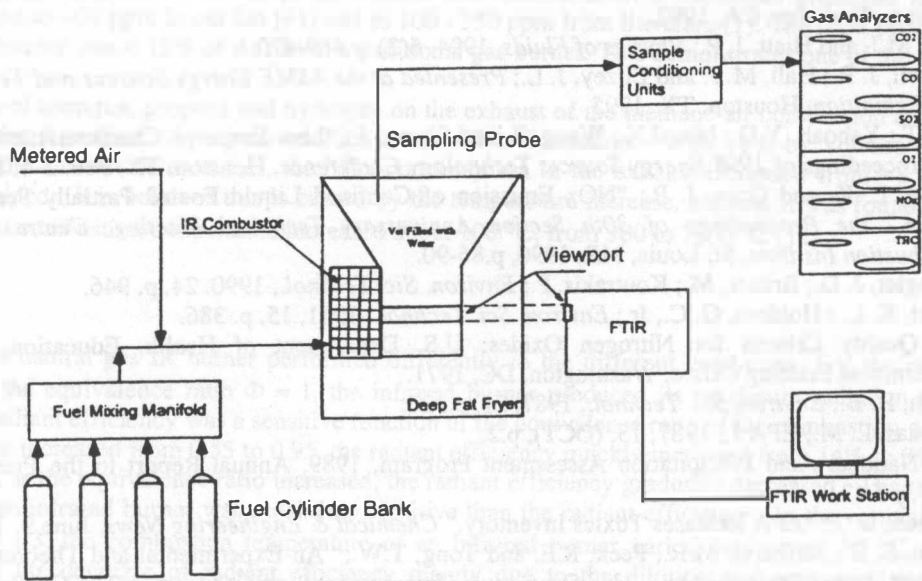


Fig. 1 A schematic of the experimental set-up.

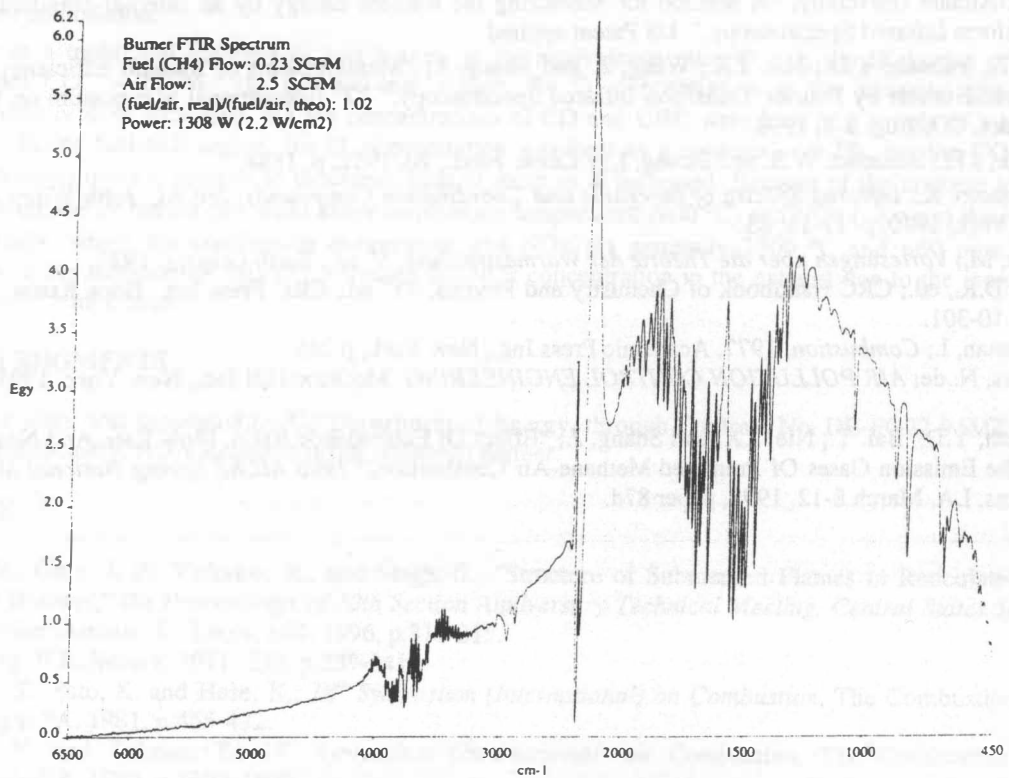


Fig. 2 Fourier transform infrared spectrum of the infrared burner.

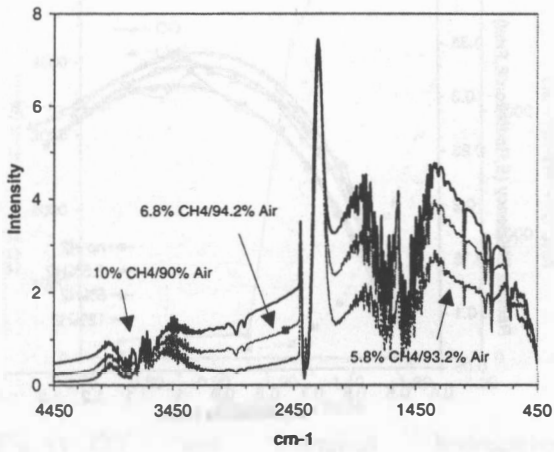


Fig. 3 FTIR spectra of the infrared burner at different methane/air ratios (methane flow 8.0 dm³/min).

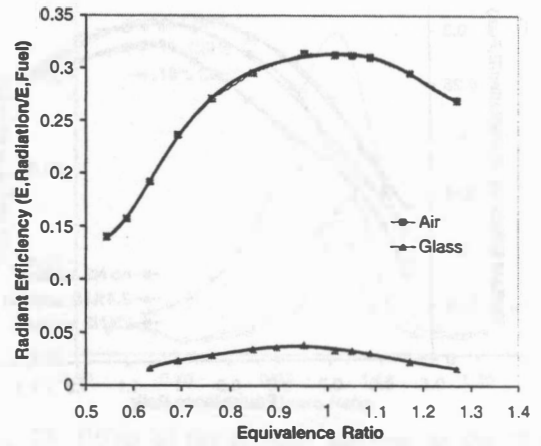


Fig. 5 Relationship of the radiant efficiency (the measured radiant energy / the total input fuel energy) and the equivalence ratio (the actual fuel-air ratio / the theoretical fuel-air ratio) for the methane-air combustion.

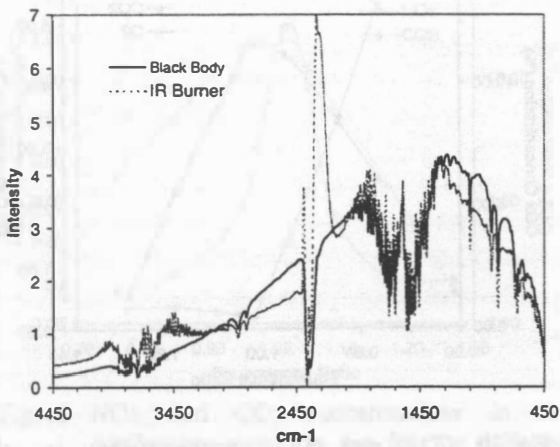


Fig. 4 FTIR spectra of the blackbody (2.03 W/cm²) and the infrared burner (methane-air, 2.2 W/cm²).

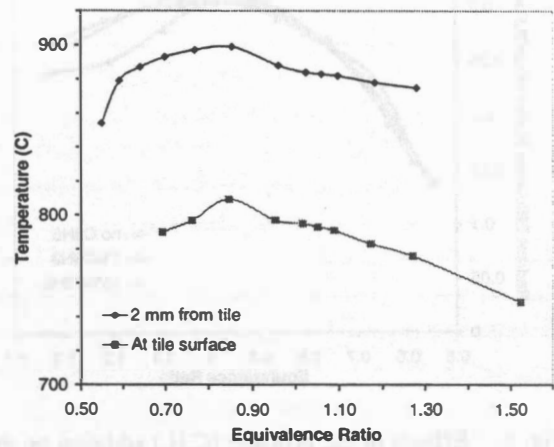


Fig. 6 The temperature profiles of the infrared radiant burner for the different equivalence ratios (8.0 dm³/min of methane).

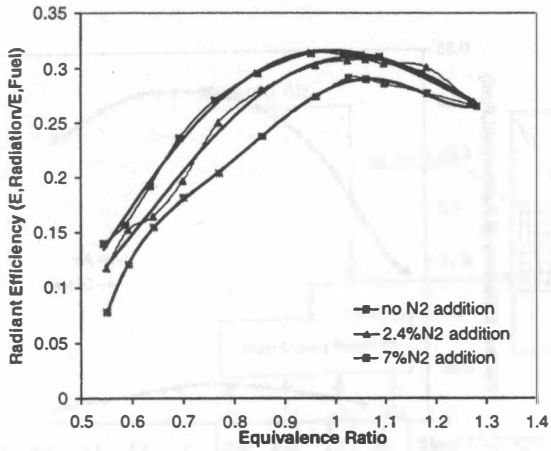


Fig. 7 Effects of the N_2 addition on the radiant efficiency.

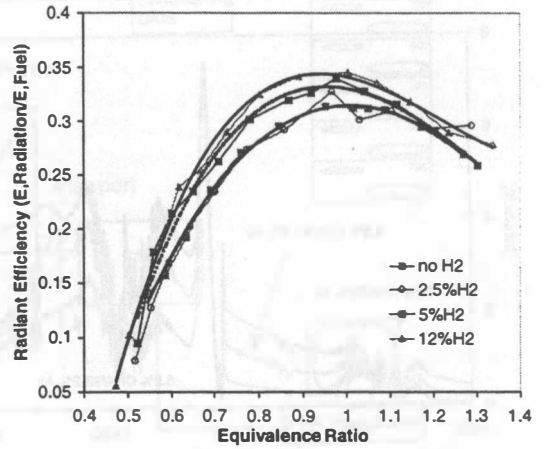


Fig. 9 Effects of the H_2 addition on the radiant efficiency.

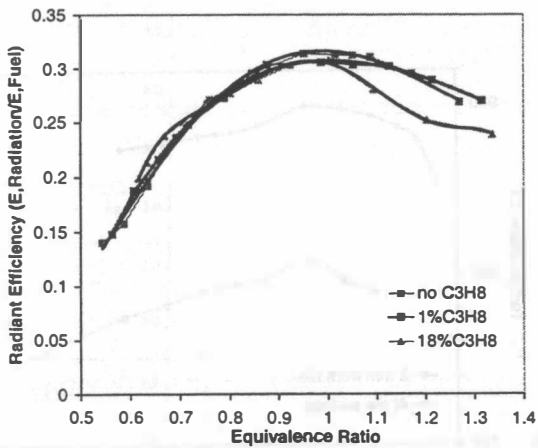


Fig. 8 Effects of the propane (C_3H_8) addition on the radiant efficiency.

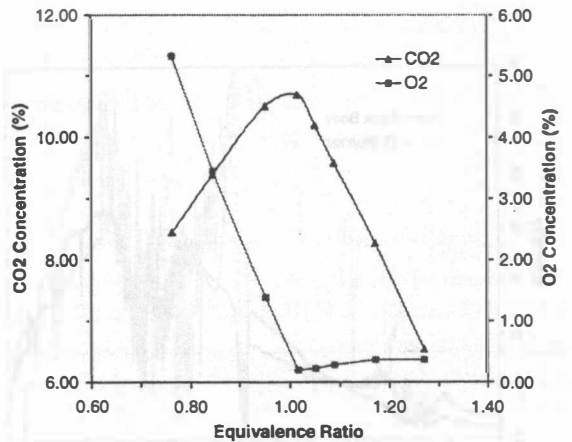


Fig. 10 CO_2 and O_2 concentrations in the combustion emission gas for the different equivalence ratio (methane + air).

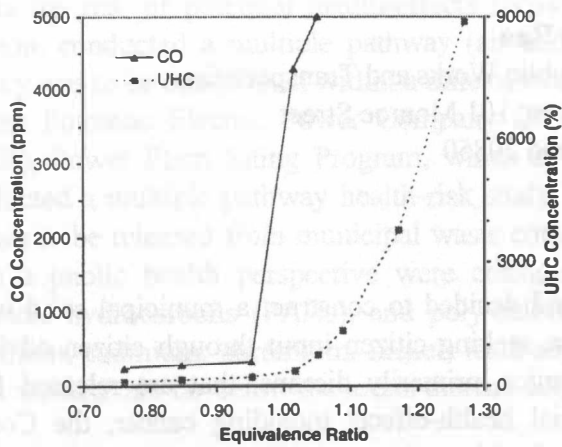


Fig. 11 CO and unburned hydrocarbon concentrations in the combustion emission gas for the different equivalence ratio (methane + air).

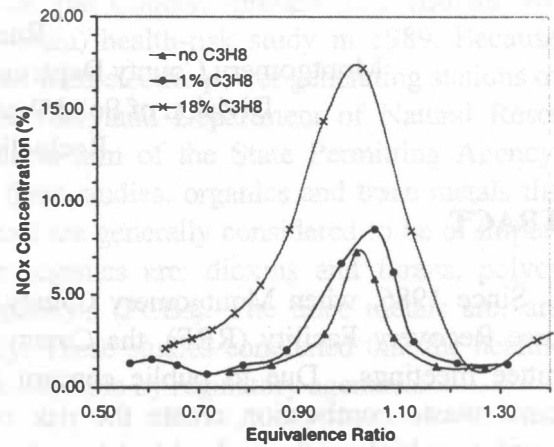


Fig. 13 Effect of the propane addition on the NOx concentration in the combustion emission gas.

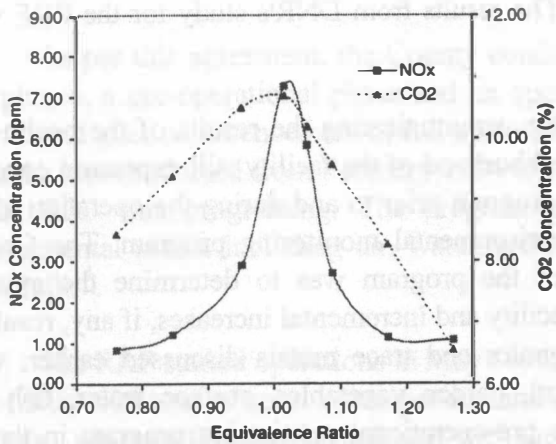


Fig. 12 NOx and CO₂ concentrations in the combustion emission gas for the different equivalence ratio (methane + air).